

## Intramolecular Amide Stacking and Its Competition with Hydrogen Bonding in a Small Foldamer

William H. James III,<sup>†</sup> Christian W. Müller,<sup>†</sup> Evan G. Buchanan,<sup>†</sup> Michael G. D. Nix,<sup>†,#</sup> Li Guo,<sup>‡</sup> Luke Roskop,<sup>§</sup> Mark S. Gordon,<sup>§</sup> Lyudmila V. Slipchenko,<sup>†</sup> Samuel H. Gellman,<sup>‡</sup> and Timothy S. Zwier<sup>\*,†</sup>

Department of Chemistry, Purdue University, West Lafayette, Indiana 47907, Department of Chemistry, University of Wisconsin, Madison, Wisconsin 53706, and Department of Chemistry, Iowa State University, Ames, Iowa 50011

Received July 3, 2009; E-mail: Zwier@purdue.edu

Protein secondary structures, including  $\beta$ -sheets,  $\alpha$ -helices, and reverse turns, generally feature networks of NH...O=C hydrogen bonds between backbone amide groups. Non-hydrogen bonded attractive interactions can be envisaged as well, based on the large dipole moment associated with the amide group ( $\mu_{\text{amide}} = 3.7 \text{ D}$ )<sup>1</sup> and the prospect of dispersion involving amide  $\pi$ -electrons. These two factors would seem to favor stacking interactions in which the amide groups are oriented in an antiparallel fashion. This mode of amide–amide interaction, however, has received relatively little attention,<sup>2–10</sup> in part because it is more difficult to detect. Formation of an H-bond is often clearly detectable by methods such as infrared or nuclear magnetic resonance spectroscopy, and there are well-established guidelines for inferring the existence of H-bonds in crystal structures. In contrast, no general spectroscopic signatures have yet been associated with non-H-bonding interactions between amide groups. Here a combined experimental and computational approach is used to identify and characterize an antiparallel amide–amide stacking interaction that arises in a small foldamer.

We have taken advantage of the amide–amide spacing in the  $\gamma$ -peptide backbone to obtain experimental evidence for face-to-face amide stacking that is competitive with intramolecular H-bonding. In Ac- $\gamma^2$ -hPhe-NHMe (Figure 1, inset), the three-carbon spacing between the amide groups enables the two planar amide groups to approach one another in a parallel (“stacked”) geometry with the amide dipoles antialigned. Single-conformation infrared and ultraviolet spectroscopy reveal signatures of this amide stacking interaction, which is particularly evident in the strong coupling between the antialigned C=O groups.

The experimental methods (SI) used to record single-conformation ultraviolet and infrared spectra of the isolated molecule cooled in a supersonic expansion are similar to those recently employed by several groups to study small polypeptides composed of  $\alpha$ -amino acid,<sup>11</sup>  $\beta$ -amino acid,<sup>12,13</sup> or a combination of  $\alpha$ - and  $\beta$ -amino acid units.<sup>14</sup> We studied Ac- $\gamma^2$ -hPhe-NHMe as a prototypical  $\gamma$ -peptide because it contains only two amide groups and bears an aromatic ring in the side chain, which is necessary for IR–UV double resonance studies. Resonant two-photon ionization (R2PI) was used to record ultraviolet spectra in a mass-selective fashion, thereby avoiding interference from thermal decomposition products. The top trace of Figure 1 shows the R2PI spectrum of Ac- $\gamma^2$ -hPhe-NHMe in the  $S_0$ – $S_1$  origin region of the phenylalanine moiety. Two of the conformers have origin transitions that are similar in intensity, A (37584  $\text{cm}^{-1}$ ) and B (37484  $\text{cm}^{-1}$ ), which dominate the R2PI spectrum. The origin transition of the third conformer, C

(37471  $\text{cm}^{-1}$ ), is significantly weaker in intensity than the other two; however, despite the intensity difference, C plays an important role in the conformational behavior of Ac- $\gamma^2$ -hPhe-NHMe.

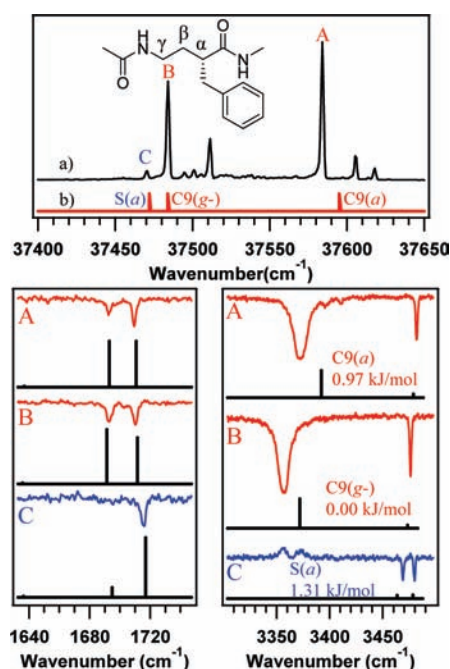


**Figure 1.** Top: (a) R2PI spectrum and (b) scaled, single-point TDDFT M05–2X/6-31+G(d) vertical excitation energies of Ac- $\gamma^2$ -hPhe-NHMe. Bottom: RIDIR spectra in the amide I (left) and amide NH stretch (right) spectral regions for the three conformers of Ac- $\gamma^2$ -hPhe-NHMe, with M05–2X/6-31+G(d) scaled, harmonic vibrational frequencies, infrared intensities (as sticks), and relative energies included for comparison (scale factors: 0.96 for amide I and 0.94 for amide NH stretch spectral regions). Table S1 contains the experimental and calculated frequencies and intensities for the data shown in Figure 1.

Once identified, these transitions can be used as monitor transitions to record resonant ion-dip infrared (RIDIR) spectra, an IR–UV double resonance method by which single-conformation infrared spectra can be obtained. The bottom panels of Figure 1 show the conformation-specific RIDIR spectra of conformers A–C in the amide I and amide NH stretch spectral regions. Based on the similarities of the infrared spectra of A and B, we conclude that the conformations responsible for these spectra are quite similar, containing a single, strong intramolecular amide–amide hydrogen bond, as evidenced by the broad NH stretch transitions shifted down in frequency to  $\sim 3360 \text{ cm}^{-1}$  in both spectra. The weak, sharp NH stretch transitions at 3481 and 3476  $\text{cm}^{-1}$  in A and B, respectively, are due to the amide NH groups not involved in the H-bond.

<sup>†</sup> Purdue University.

<sup>#</sup> Present address: University of York, York, UK.

<sup>‡</sup> University of Wisconsin–Madison.

<sup>§</sup> Iowa State University.

Conformers A and B also show nearly identical spectra in the amide I region, as expected based on the similar H-bonding in both structures.

Stick diagrams showing scaled harmonic vibrational frequencies and infrared intensities of the NH stretch modes calculated at the DFT M05-2X/6-31+G(d) level of theory<sup>15,16</sup> are included in Figure 1 for comparison with experiment. The computed spectra faithfully reproduce the experimental spectra of all three conformers, leading to firm structural assignments. Conformers A and B are both ascribed to a family of structures containing a nine-atom ring (C9) that is closed by an NH...O=C H-bond (Figure 2, top panel). The two structures differ in the position of the phenyl ring relative to the peptide backbone, gauche (*g-*) for conformer B and anti (*a*) for conformer A.

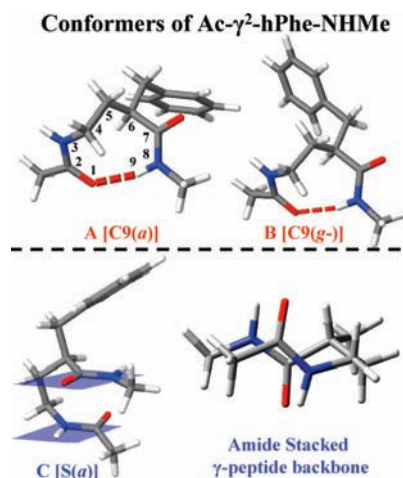


**Figure 2.** M05-2X/6-31+G(d) optimized geometries of Ac- $\gamma^2$ -hPhe-NHMe. Top: The two C9 H-bonded conformers ascribed to A and B (dashed lines in red denote the intramolecular amide–amide hydrogen bond). Bottom: The amide stacked structure ascribed to conformer C (left) and an alternate view of the amide stacked interaction with the aromatic ring replaced by a hydrogen atom for clarity.

The spectra of conformer C in the amide NH stretch and amide I regions provide a striking contrast to those of A and B. Both NH stretch fundamentals of C occur at frequencies characteristic of non-H-bonded amide NH groups (3469 and 3480  $\text{cm}^{-1}$ ). The gains in the RIDIR spectrum of C (3357, 3372  $\text{cm}^{-1}$ ) (Figure 1C) are the result of an IR-created background that contributes to the R2PI signal at the UV wavelength used to monitor conformer C, when the strong H-bonded NH stretch fundamentals of conformers A and B are excited. In the amide I spectral region, the spectrum displays a single, dominant transition at 1716  $\text{cm}^{-1}$ , despite the presence of two C=O groups in the molecule. Calculations clearly point to a structure for conformer C in which the carbonyl groups are antialigned and strongly coupled, producing in-phase and out-of-phase oscillations that enhance the intensity in one fundamental at the expense of the other, leading to the assignment of C to an amide stacked structure (Figure 2, bottom). Fully extended conformers possessed vibrational frequencies and IR intensities (Figure S1) that were poorer matches to the experimental data than were those calculated for the amide stacked conformation, particularly in that the extended conformations displayed two C=O stretch fundamentals of comparable intensity.

Single-point TDDFT M05-2X/6-31+G(d) vertical excitation energies of the three conformers were used to compare experimental and theoretical  $S_0$ – $S_1$  origin frequencies. The computed frequencies for C9(*a*), C9(*g-*), and S(*a*), scaled to the experimental  $S_0$ – $S_1$  origin of conformer B (Figure 1), are in agreement with the experimental

spacing. Extended conformers were shifted more than 300  $\text{cm}^{-1}$  lower in frequency than the calculated origin of conformer B (Table S1), which argues against assignment of conformer C to an extended conformation.

Calculations predict amide stacked structures to have energies nearly as low as those due to C9 H-bonded conformations, within 2 kJ/mol of one another, a result consistent with observing both types of structures in the supersonic expansion. Extended and C7 H-bonded conformers were found to be less stable (>10 kJ/mol), which supports the assignment of the three observed conformers to C9 or amide stacked conformers.

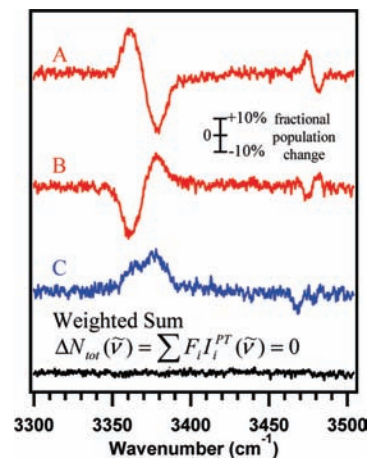


**Figure 3.** MRIRPT scans of conformers A–C of Ac- $\gamma^2$ -hPhe-NHMe in the amide NH stretch region. Dips and gains in each spectrum arise from loss or gain in population in the monitored conformation downstream caused by IR excitation upstream. The total signal level of the UV probed conformer in the absence of the IR pump pulse was set to a known output signal level, while the difference in ion signal with or without the IR laser was recorded using active baseline subtraction in a gated integrator.

A quantitative measurement of the relative abundances of amide stacked and H-bonded conformations in Ac- $\gamma^2$ -hPhe-NHMe was carried out using mass-resolved infrared population transfer spectroscopy (MRIRPT), an extension of previous population transfer spectroscopies.<sup>23</sup> MRIRPT spectra were obtained by counter-propagating the infrared laser along the molecular beam, creating a column of IR-excited molecules for interrogation. By adjusting the timing of the IR excitation relative to the UV probe laser ( $\Delta t = 44 \mu\text{s}$ ), molecules initially excited within a few millimeters of the pulsed valve orifice can isomerize and be recooled during travel to the ion source region before interrogation with the UV probe via R2PI. The ion signal due to one conformer is monitored via its  $S_0$ – $S_1$  origin transition while the IR laser is tuned through the spectral region of interest. IR transitions due to the probed conformer appear as depletions in ion signal, while gains in ion signal are observed when transitions of other conformers are encountered that transfer population into the probed conformer zero-point level. The set of MR-IRPT spectra is used to extract relative abundances by taking a weighted sum of the spectra (Figure 3, bottom) that zero-out the net change in population at all wavelengths ( $\Delta N_{\text{tot}}(\tilde{\nu}) = 0$ ). These weighting factors are the relative fractional abundances of the conformers.<sup>23</sup> The fractional abundances derived from MRIRPT give  $F_C = 0.21 \pm 0.01$ , within a factor of 2 of either of the amide–amide hydrogen bonded conformers ( $F_A = 0.38 \pm 0.01$  and  $F_B = 0.41 \pm 0.02$ ). This method avoids the use of  $S_0$ – $S_1$  origin intensities to infer relative fractional abundances (Figure 1, top), which assume identical Franck–Condon factors, excited state lifetimes, and R2PI cross sections for each conformer. The MRIRPT

abundances differ strikingly from those inferred from the intensities in the R2PI spectrum ( $I_A = 0.55$ ,  $I_B = 0.40$ ,  $I_C = 0.05$ ), pointing to significant differences in the R2PI efficiencies of the conformations.

To evaluate the various contributions to the stabilization present in the amide stacked structure, the systematic fragmentation method (SFM)<sup>17–19</sup> was used to divide the molecular structure into fragments whose nonbonded interactions can be evaluated and characterized using the effective fragment potential (EFP) method.<sup>20,21</sup> One of the strengths of the EFP method is that it allows one to apportion the nonbonded interaction energy into physically meaningful contributions, including Coulombic (electrostatics), induction (polarization), exchange repulsion, dispersion, and charge transfer.

Comparison of these contributions for the structures assigned to conformers A–C (Table 1) was carried out with the SFM internal energies calculated at the M05-2X/6-31+G(d) level of theory. As anticipated, dispersion plays a larger role in the amide stacked structure (–18 kJ/mol) than in its C9 H-bonded counterparts (–10 kJ/mol), just as it does in other circumstances in which two  $\pi$  clouds interact with one another.<sup>22</sup> Indeed, although the electrostatic term favors structures A and B by 5–7 kJ/mol, the dispersion interaction favors C by a similar amount. The electrostatic contribution from the SFM/EFP calculations is the single largest attractive contribution to amide stacking, more than 80% of that in the C9 structures, indicating that there is also a significant stabilization from the antialigned polar amide groups.

**Table 1.** Results of SFM/EFP Calculations for the Nonbonded Interactions in the Three Conformers of Ac- $\gamma^2$ -hPhe-NHMe at the M05-2X/6-31+G(d) Level of Theory

| experimental conformer assigned structure | C S(a)   | B C9(g)  | A C9(a)  |
|---|----------|----------|----------|
| Nonbonded contributions                   | (kJ/mol) | (kJ/mol) | (kJ/mol) |
| electrostatics                            | –31.58   | –38.29   | –36.63   |
| exchange repulsion                        | 36.11    | 27.32    | 25.24    |
| polarization                              | –1.94    | –7.12    | –6.55    |
| dispersion                                | –18.06   | –10.82   | –10.61   |
| charge transfer                           | –4.81    | –3.63    | –3.38    |
| Total nonbonded energy                    | –20.28   | –32.54   | –31.93   |
| Relative nonbonded energy                 | 12.26    | 0.00     | 0.61     |
| Total relative energy <sup>a</sup>        | 1.31     | 0.00     | 0.97     |
| Relative through bond energy <sup>b</sup> | –10.95   | 0.00     | –0.36    |

<sup>a</sup> Fully optimized relative energies at the M05-2X/6-31+G(d) level of theory. <sup>b</sup> Difference between total relative and relative nonbonded energies ascribable to through bond contributions to the relative stabilities.

The net nonbonded contribution to the stabilization of the stacked structure (–20.3 kJ/mol) is  $\sim$ 12 kJ/mol smaller than that in C9(g) (–32.5 kJ/mol), while the total relative energies differ by only 1.3 kJ/mol. Hence, there is a through-bond contribution that stabilizes the amide stacked structure relative to C9 structures that is not captured by the nonbonded EFP energy. This factor arises from strain in the three-carbon bridge between amide groups; this strain is minimized in the amide stacked conformation. In contrast,

formation of the intramolecular H-bond in the C9 structures induces some torsional strain in the segment linking the two amide groups.

In conclusion, the  $\gamma$ -peptide backbone juxtaposes adjacent amide groups in a way that facilitates amide stacking, an interaction that is energetically competitive with nearest-neighbor H-bonding. Single-conformation IR spectra in the NH stretch and amide I regions show clear evidence for a planar stacked conformation in which the amide groups are antialigned. In the case of  $\gamma$ -peptide foldamers, amide stacking can be used as a design element for conformational control, a strategy that could lead to unique secondary structures not yet anticipated.

**Acknowledgment.** W.H.J., C.W.M., E.G.B., M.G.D.N., T.S.Z. (NSF-CHE0909619), L.G., and S.H.G. (CHE-0848847) acknowledge support from the NSF. L.V.S. acknowledges support from Purdue University. L.R. and M.S.G. acknowledge support from the Air Force Office of Scientific Research.

**Supporting Information Available:** Complete ref 16. Experimental and computational methods, conformational analysis details. This material is available free of charge via the Internet at <http://pubs.acs.org>.

## References

- (1) Cantor, C. R.; Schimml, P. R. *Biophysical Chemistry: I. The Conformation of Biological Macromolecules*; W. H. Freeman and Co.: San Francisco, 1980.
- (2) Choudhary, A.; Gandla, D.; Krow, G. R.; Raines, R. T. *J. Am. Chem. Soc.* **2009**, *131*, 7244.
- (3) Yonezawa, T.; Morishim., I. B. *Chem. Soc. Jpn.* **1966**, *39*, 2346.
- (4) Rabinovitz, M.; Pines, A. *J. Chem. Soc. B* **1968**, 1110.
- (5) Betson, M. S.; Clayden, J.; Lam, H. K.; Helliwell, M. *Angew. Chem., Int. Ed.* **2005**, *44*, 1241.
- (6) Clayden, J. *Chem. Soc. Rev.* **2009**, *38*, 817.
- (7) Maccallum, P. H.; Poet, R.; Milnerwhite, E. J. *J. Mol. Biol.* **1995**, *248*, 361.
- (8) Maccallum, P. H.; Poet, R.; Milnerwhite, E. J. *J. Mol. Biol.* **1995**, *248*, 374.
- (9) Hinderaker, M. P.; Raines, R. T. *Protein Sci.* **2003**, *12*, 1188.
- (10) Fischer, F. R.; Wood, P. A.; Allen, F. H.; Diederich, F. P. *Proc. Natl. Acad. Sci. U.S.A.* **2008**, *105*, 17290.
- (11) Chin, W.; Piuze, F.; Dimicoli, I.; Mons, M. *Phys. Chem. Chem. Phys.* **2006**, *8*, 1033.
- (12) Baquero, E. E.; James, W. H.; Choi, S. H.; Gellman, S. H.; Zwier, T. S. *J. Am. Chem. Soc.* **2008**, *130*, 4784.
- (13) Baquero, E. E.; James, W. H.; Choi, S. H.; Gellman, S. H.; Zwier, T. S. *J. Am. Chem. Soc.* **2008**, *130*, 4795.
- (14) James, W. H.; Baquero, E. E.; Shubert, V. A.; Choi, S. H.; Gellman, S. H.; Zwier, T. S. *J. Am. Chem. Soc.* **2009**, *131*, 6574.
- (15) Zhao, Y.; Truhlar, D. G. *J. Chem. Theory Comput.* **2007**, *3*, 289.
- (16) Frisch, M. J., *Gaussian 03*, revision E.01; Gaussian, Inc.: Wallingford, CT, 2004.
- (17) Deev, V.; Collins, M. A. *J. Chem. Phys.* **2005**, *122*, 154102.
- (18) Gordon, M. S.; Mullin, J. M.; Pruitt, S. R.; Roskopf, L. B.; Slipchenko, L. V.; Boatz, J. A. *J. Phys. Chem. B* **2009**, *113*, 9646.
- (19) Schmidt, M. W.; Baldrige, K. K.; Boatz, J. A.; Elbert, S. T.; Gordon, M. S.; Jensen, J. H.; Koseki, S.; Matsunaga, N.; Nguyen, K. A.; Su, S. J.; Windus, T. L.; Dupuis, M.; Montgomery, J. A. *J. Comput. Chem.* **1993**, *14*, 1347.
- (20) Gordon, M. S.; Freitag, M. A.; Bandyopadhyay, P.; Jensen, J. H.; Kairys, V.; Stevens, W. J. *J. Phys. Chem. A* **2001**, *105*, 293.
- (21) Gordon, M. S.; Slipchenko, L. V.; Li, H.; Jensen, J. H. *Ann. Rep. Comput. Chem.* **2007**, *3*, 177.
- (22) Slipchenko, L. V.; Gordon, M. S. *J. Comput. Chem.* **2007**, *28*, 276.
- (23) Dian, B. C.; Longarte, A.; Winter, P. R.; Zwier, T. S. *J. Chem. Phys.* **2004**, *120*, 133.

JA9054965